Unveiling High Performance Solder Alloys for Automotive Applications

Pritha Choudhury, Raghu Raj Rangaraju, Morgana Ribas, Siuli Sarkar

MacDermid Alpha Electronics Solutions

Bangalore, India

Email: Pritha.Choudhury@MacDermidAlpha.com

Paul Salerno, Alan Plant

MacDermid Alpha Electronics Solutions

South Plainfield, NJ, USA

Paul.Salerno@MacDermidAlpha.com

Abstract

Vehicle electrification and advances in autonomous driving technologies are creating unique opportunities and challenges in the automotive electronics assembly industry. The ever-increasing demand of reliability at higher temperatures and longer service life, especially for automotive electronics, is leading to the evolution of high reliability solder alloy design in the electronics assembly industry. The combination of harsh operating conditions, increasing power densities, and miniaturization has added to the complexity of assembly designs in the automotive electronics market for which traditional surface mount solders are no longer applicable. Thermo-mechanical reliability of solder alloys under harsh operating conditions has been a primary factor for defining suitability and selection of solder alloy for next generation designs. A next generation high reliability alloy for automotive electronics is introduced herein. The microstructure of this novel alloy consists of a well-distributed eutectic phase and finely distributed precipitates of intermetallic compounds which contributes towards solid solution strengthening as well as precipitation strengthening. It is shown that a high-temperature superior creep strength improvement of more than 100% over existing high reliability alloys is achieved at temperatures of 150°C. This and other mechanical properties of the bulk alloy are then correlated to performance with thermal cycling testing under extreme conditions. The novel alloy showed significantly higher thermal cycling performance, exhibiting more than 40% increase in the characteristic life over other existing high-reliability alloys while maintaining traditional surface mount target reflow temperatures. Considering these results, this new class of alloys has the capability to meet the increasingly challenging reliability requirements of automotive electronics.

Key words

Automotive, Creep, High reliability, Microstructure.

I. Introduction

Environmental concerns, regulatory requirements, alloy properties and business best practices have been key drivers for the development of solder alloys for electronic assembly since the transition to lead-free solders [1- 3]. More recently, there is a growing demand for solders that can address emerging applications of electronics in more challenging operating conditions such as higher operating temperature or extended service life [4 - 8]. The upcoming transition to electric vehicles and a trend towards autonomous driving are creating further growth opportunities and challenges in the automotive electronics industry to ensure electronic devices are continually operating for extended periods of time. There has been an accelerated growth in the number and complexity of electronics in vehicles ranging from safety devices to complete autonomous vehicles where there is a clear requirement for higher processing power in more

compact designs [6-7]. Increasingly, the electronic controls and sensors in automotive vehicles must work in high-temperature environments. The need for efficient power dissipation in hybrid and fuel cell electric vehicles will further increase the demand for high-temperature power electronics [7]. Harsh thermal conditions of an under-the-hood automobile environment require sophisticated design methods, materials, and tools to give reliable and cost-effective packaging [6]. Similarly, there may be cases in which interconnects are also exposed to high junction temperatures.

The coefficient of thermal expansion (CTE) mismatch between the substrate and solder joints or solder joint and package is well-documented. When the assembly undergoes changes in temperature,often correlated to thermal cycling test, solder interconnects are subjected to cyclic stresses due to CTE mismatch and may fail due to creep/thermomechanical fatigue. The mechanism of damage during thermomechanical fatigue is likely to be the same as during creep deformation. The corresponding damage accumulates in the solder rather than in the components to which it is joined, so the solder joint properties are of uttermost interest. If the solder is unable to accommodate the creep damage, the joined components will deform or fracture over time.

In response to the above requirements of automotive electronics, new high performance solder alloys have been developed. The combination of two key strengthening mechanisms of the alloy microstructure is shown here to increase thermomechanical fatigue life: solid solution and precipitation strengthening. Bi, In and Sb form solid solution with Sn, having high solubility in the Sn matrix, which does not vary significantly at higher temperatures. Therefore, the strength of the alloy is retained even at high operational temperatures. On the other hand, Ag and Cu have limited solubility in Sn, leading to the formation of Ag_3Sn and Cu_6Sn_5 intermetallic compounds. A fine distribution of these intermetallic compounds suppresses the plastic deformation and propagation of cracks formed during thermal cycling. Other micro-additives (up to a maximum of 0.5 wt. %), can form finely distributed intermetallic compounds that enhance the strength of the alloys. Additional metallurgical methods such as grain refinement and diffusion modifiers help optimize the properties of these alloys and their corresponding solder joints and are discussed elsewhere.

This research effort seeks to characterize two high reliability solder alloys using uniaxial tensile tests, high temperature creep tests and CTE measurements. High thermal fatigue resistance can be achieved by improving high temperature creep resistance in solder alloys, such as by combining solid solution strengthening and precipitation/ dispersion hardening of the tin matrix [9 - 10]. Bi and Sb are elements with higher solid solubility in Sn which can contribute, in various degrees, towards solid solution strengthening of the Sn matrix.

II. Experimental Procedure

The alloys used in this study have a wide range of compositions including Sb and Bi additions and a generic description is shown in Table I. These alloys are Sn-Ag-Cu based, having Sb additions in varying proportions and Bi addition between 20 and 50% of Sb. These alloys contain up to two minor alloying additions (generically referred as X) that make up less than 0.5 wt.% of the alloy composition. The properties of the new alloys are compared with that of an existing high reliability alloy (High Rel Alloy) and discussed with respect to their respective microstructure.

Table I: Generic description of the alloys.

Alloy ID	**Generic Description**
High Rel Alloy	Sn-Ag-Bi-Sb-Cu-Ni
Alloy 10	Sn-Ag-Bi-Sb-Cu-X
Alloy 39	Sn-Ag-Bi-Sb-Cu-X

Alloys were prepared using conventional liquid metallurgy route, at a superheat of 50ºC. Compositions were analyzed using OES and/or ICP-OES, and the melting behavior was studied using a differential scanning calorimeter (DSC) as per ASTM E794 standard using a heating rate of 10^0C/min.
The microstructure of the alloys weas studied using a scanning electron microscope (SEM). The elements present in the alloys were also identified using Energy Dispersive X-Ray Spectroscopy (EDS).
Tensile tests were carried out using a universal testing machine (Model 5566), and specimens were prepared as per ASTM E8 tensile test standard. Circular specimens of 24 mm gage length (L), 6 mm gage diameter (D), and 6 mm shoulder radius (R) (Fig. 1) were used for the tests. Tests were performed at two temperatures, 25ºC and 125ºC, and strain rate 10^{-3} s^{-1} corresponding to crosshead speed of 1.44 mm/min.
A microhardness tester was used to measure hardness at an applied load of 1 kg. CTE was measured using a thermal mechanical analyzer, as per the RT-500C standard. A scan rate of 10ºC/ min in the temperature range of 30 to 150ºC was used.

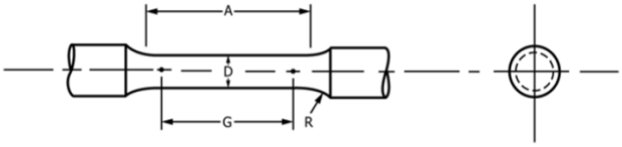

Fig. 1: Specimen geometry for tensile tests.

For the creep test, round-threaded samples with 9 mm gage length and 6 mm diameter were machined as shown in Fig. 2. Samples were cleaned with IPA and heat treated at 125°C for 48 hours prior to testing. Creep tests were performed at 150°C and 200N load considering the end-use condition of these alloys.

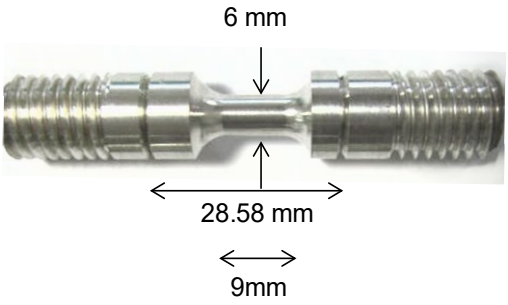

Fig. 2: Specimen for creep test

Elastic properties were measured using the ultrasonic pulse-echo technique through computations based on measured sound velocities and material density. An ultrasonic thickness gage and appropriate transducers are used to measure the longitudinal and shear wave velocities through the alloys.

The alloys were processed into type 4 powder (refer to IPC J-STD-006A standard for details) and mixed into a paste using an appropriate paste flux for further reliability evaluation. The proportion between powder and paste flux was such that an 88.5% metal loading was achieved. The reflow profile shown in Fig. 3, consisted of soaking for 60-90 seconds at 150-160°C. The time above liquidus (TAL) 230°C was 60 seconds while the reflow peak temperature was 245°C.

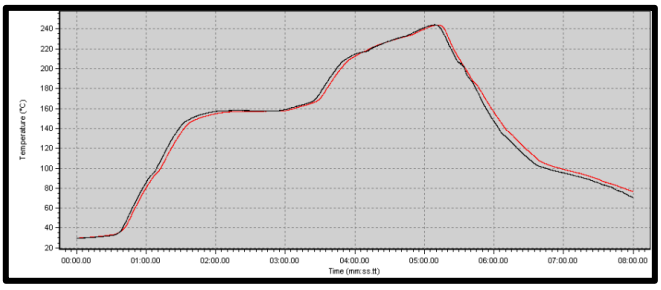

Fig. 3: Reflow profile

Thermal fatigue tests were carried out using an air-to-air thermal cycling chamber, in which the samples were cycled from -40 to +150°C, with 30 minutes dwell time at each temperature for a total of 2500 cycles. This harsh test profile involves a large transition of 190°C in every cycle that lasts for 75 minutes (including transition times). The board used for thermal reliability test has Cu OSP finish and consists of four different components, as described in Table II. An increase of 20% in electrical resistance above the initial values, for five consecutive readings, was considered as a failure, as per IPC-9701A standard [11].

Table II: Details of Components

Component	Body Size	Pitch	Ball Matrix/ Lead Count	Ball Alignment
CTBGA228	12 mm x 12 mm	0.5 mm	22 x 22	Perimeter
CABGA256	17 mm x 17 mm	1.0 mm	16 x 16	Full Array
MLF52	8 mm x 8 mm	0.5 mm	52	NA
MLF100	12 mm x 12 mm	0.4 mm	100	NA

III. Results and Discussion

A. Microstructure and Physical Properties

The microstructures of the as-cast alloys and the corresponding powders are shown in Fig. 4. The microstructure of the alloys show characteristic Ag_3Sn eutectic and $(Cu,Ni)_6Sn_5$ precipitates dispersed in the Sn matrix, and the respective powders are of regular morphology. Other intermetallic compounds are refined and well-dispersed in the microstructure. The Sb-Sn phase is observed in close association with the eutectic phase, demonstrating one of the mechanisms for strengthening the matrix.

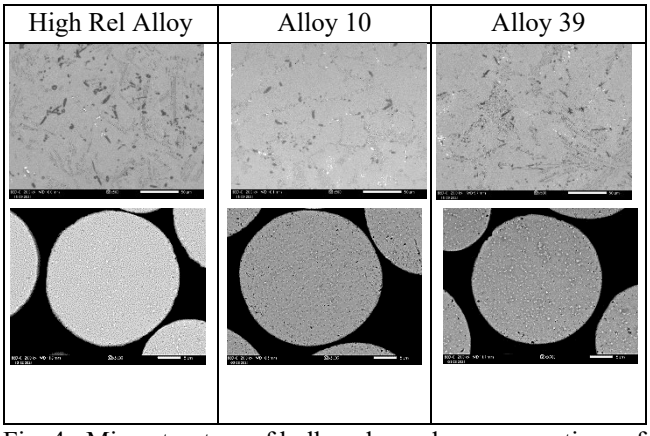

Fig. 4: Microstructure of bulk and powder cross-sections of the alloys.

B. Mechanical and Physical Properties

The physical properties of all the alloys are listed in Table III. The melting behavior, viz. solidus and liquidus

temperatures, is a decisive property for guiding high temperature reliability of solders. However, changes in alloy composition for achieving that need to be carefully conducted to avoid drastically reducing the corresponding solder joint thermal reliability. Higher Sb content in Alloy 10 and Alloy 39 have increased the liquidus temperatures in both alloys compared to the High Rel Alloy. The moduli of the new alloys are lesser than the existing High Rel Alloy, thus making them less stiff that is likely to help in improving the thermal fatigue resistance.

The variation of tensile strength and yield strength with temperature is shown in Fig. 5. An increase of 34% tensile strength is achieved in the new alloys at 125^{0}C. The retention of high strength at the higher operating temperature is expected to translate into higher thermomechanical fatigue resistance.

Table III: Properties of all alloys

Properties	**Alloys**		
	High Rel Alloy	**Alloy 10**	**Alloy 39**
Melting Range (°C)	212-220	217-229	213-226
Density (gm/cm^3)	7.5	7.4	7.4
Hardness (HV-1)	27.2	27.0	28.4
CTE (µm/mK) (30-100°C)	24.8	25.0	24.5
CTE (µm/mK) (100-150°C)	27.4	26.7	26.1
Young's Modulus (GPa)	52.0	41.0	47.4
Shear Modulus (GPa)	19.1	14.6	17.2
Poisson's Ratio	0.36	0.40	0.38
Thermal Conductivity (W/mK)	55.2	49.1	46.2

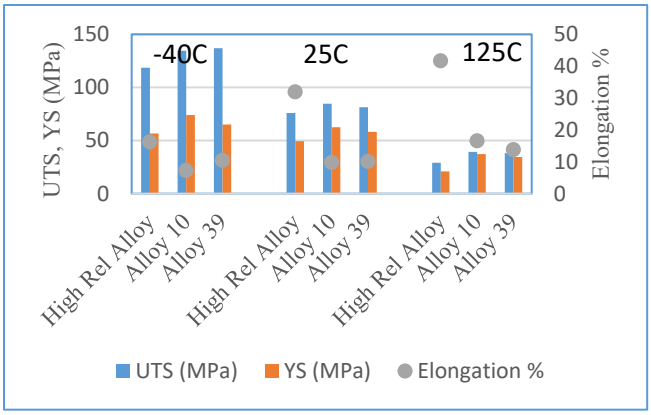

Fig. 5: Effect of temperature on uniaxial tensile properties

C. Creep and Thermomechanical Fatigue

Creep properties, i.e., creep rupture time and creep elongation, of the alloys are shown in Fig. 6. During the high temperature creep test, the specimens are subjected to stresses lower than their respective yield stresses, but they fail due to accumulated degradation caused by various mechanisms. At 150°C, the homologous temperature of the High Rel Alloy, and alloys 10 and 39 is 0.86, 0.84 and 0.85, respectively. So, the deformation is time-dependent and controlled by creep.

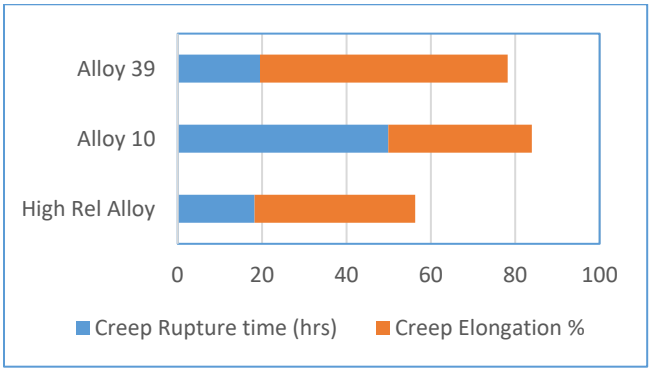

Fig. 6: Creep properties of the alloys

The very harsh thermal cycling profile combined with the small pitch of BGA228 resulted in enough failures in this component to enable plotting a Weibull curve, which is shown in Fig. 7. The characteristic life of Alloy 39 and Alloy 10 improves by more than 40%, while first failure and 1% failure occur later than the existing High Rel. Alloy. During thermal cycling, the solder interconnections ultimately fail from creep fatigue as they are subjected to cyclic stresses due to the coefficient of thermal expansion (CTE) mismatch between component and printed circuit board. Ultimately, if the solder alloy is unable to accommodate the creep damage, the solder joints will deform or fracture. The high creep strength of Alloy 10 has helped in accommodating the damage due to creep resulting in high characteristic life

during thermal cycling. The ability of Alloy 39 to undergo high elongation during creep helps in absorbing the cyclic strains generated during thermal cycling. Both these alloys have at least 67% higher yield strength than the High Rel Alloy at elevated temperature as shown in figure 5. The higher yield strength enables these alloys to resist plastic deformation to a greater extent than the High Rel Alloy. Thus, the right combination of improved bulk mechanical properties in two new alloys have resulted in up to 56% increase in characteristic life of BGA228 components in a very harsh thermal cycling profile.

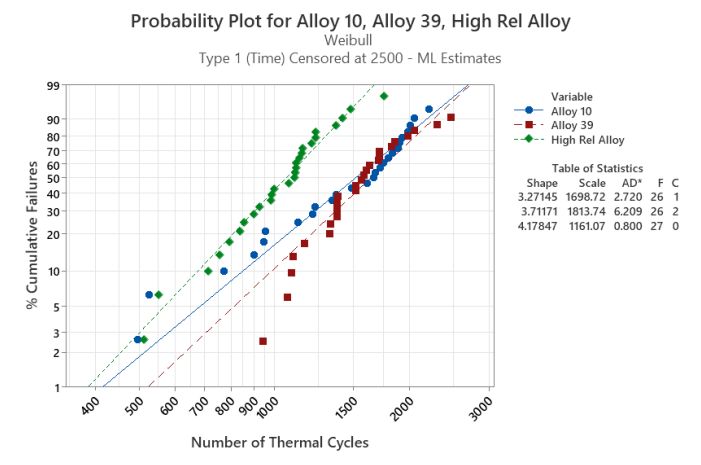

Fig. 7: Weibull plot of BGA228 failures

III. Conclusion

High reliability lead-free solder alloys are strongly desirable, especially as the automotive industry migrates to electric vehicles and autonomous driving that require extended service life in high operating temperature environments. We show here that high temperature tensile and creep properties can be used as an indicator for the long-term thermo-mechanical reliability of such alloys. Key conclusions are:

- Strengthening mechanisms such as solid solution and precipitation strengthening, induced by a suitable choice of micro additives are used to achieve the desirable properties.
- Micro-alloying additions contribute to intermetallic compounds formation and strength retention at high temperatures.
- More than 100% improvement in creep strength and 50% increase in creep elongation over that of the existing High Rel Alloy have been achieved by the novel alloys presented here.
- An increase in characteristic life by 56% and 46% is observed in Alloy 39 and Alloy 10, respectively, over that of the existing High Rel Alloy on a BGA228 package.
- The new alloys provide practical suitability for use in electronic applications demanding extended service life when exposed to high temperature environments.

➢ Next on studies:
- Investigation on the vibration resilience of the alloys.

References

[1] Iver E. Anderson, et. al, "Effects of Alloying in Near-Eutectic Tin-Silver-Copper Solder Joints", Materials Transactions, **vol. 43**, no.8 (2002), pp. 1827-1832

[2] A.A. El-Daly and A.E. Hammad, "Development of high strength Sn–0.7Cu solders with the addition of small amount of Ag and In" J. of Alloys and Compounds, **509** (2011), pp. 8554-8560.

[3] Peter Zimprich, Usman Saeed, Agnieszka Betzwar-Kotas, Brigitte Weiss and Herbert Ipser, "Mechanical Size Effects in Miniaturized Lead-Free Solder Joints", J. of Electronic Materials, **vol. 37**, no.1 (2008), pp. 102-109.

[4] Carina Morando, Osvaldo Fornaro, Olga Garbellini and Hugo Palacio, "Thermal properties of Sn-based solder alloys", J. Mater. Sci.: Mater Electron, **vol 25** (2014) pp 3440-3447.

[5] R. W. Johnson and P. Jacobsen, "The changing automotive environment: high temperature electronics". IEEE Transactions on Electronics Packaging Manufacturing, **vol. 27** (3), pp.164-176, 2004.

[6] Walter L. Winterbottom, "Converting to lead-free solders: An automotive industry perspective". JOM, **vol. 45** (7), pp. 20-24, 1993.

[7] Alexandrine Guedon, Eric Woirgard, Christian Zardini, "Evaluation of Lead-free Soldering for Automotive Applications", Microelectronics Reliability, **vol 42** (2002), 1555-1558.

[8] Jung-Hwan Bang, Dong-Yurl Yu, Young-Ho Ko, Jeong-Won Yoon and Chang-Woo Lee, "Lead-free Solder for Automotive Electronics and Reliability Evaluation of Solder Joint", J. of Welding and Joining, **vol. 34**, no. 1 (2016), pp 26-34

[9] E. Lechovic, E. Hodulova, B. Szewczykova, I. Kovarikova, K. Ulrich, "Solder Joint Reliability". Institute of Production Technologies, Faculty of Materials Science and Technology, Slovak Institute of Technology, pp. 1-8.

[10] P. Choudhury et al., "New lead-free alloy for high reliability, high operating temperature conditions". Proceedings of the ICSR (Soldering and Reliability) Conference, September 2014.

[11] "Performance Test Methods and Qualification Requirements for Surface Mount Solder Attachments", IPC- 9701A, IL, USA (2006)